Lawrence Berkeley National Laboratory

Title
INTERPRETATION OF NONISOTHERMAL STEP-RATE INJECTION TESTS

Permalink
https://escholarship.org/uc/item/23n2c044

Author
Benson, S.

Publication Date
1982-12-01

Lawrence Berkeley Laboratory
UNIVERSITY OF CALIFORNIA

EARTH SCIENCES DIVISION

INTERPRETATION OF NONISOTHERMAL STEP-RATE
INJECTION TESTS

S. Benson

December 1982

DISCLAIMER

Interpretation of Nonisothermal Step-Rate Injection Tests

Sally Benson
Earth Sciences Division
Lawrence Berkeley Laboratory
University of California
Berkeley, California 94720

INTRODUCTION

Injection tests are a common method of obtaining well and reservoir data in geothermal wells. Invariably the temperature of the injected fluid is different than that of the reservoir fluid. Because of the strong temperature dependence of fluid viscosity, and to a lesser extent, fluid density; nonisothermal related pressure transients must be considered to correctly interpret the data. Recent studies of single rate nonisothermal injection have shown that the pressure transients can be classified by one of two cases: 1) a moving thermal front dominated problem or 2) a composite reservoir problem. Analysis methods to determine the permeability thickness of a reservoir and the skin factor have been developed for both of these cases by Benson and Bodvarsson[1]. This paper discusses the extension of these methods to step-rate injection tests and proposes a new method for tracking thermal fronts in injection wells.

BACKGROUND

Several authors have discussed the interpretation of pressure transients during cold water injection into hot reservoirs. In particular, Bodvarsson and Tsang[2] and Mangold et al[3] demonstrated the behavior of nonisothermal pressure transients in geothermal reservoirs and illustrated the effect of the temperature dependent fluid properties, viscosity and density. Tsang and Tsang[4] developed a semi-analytic solution for pressure transients during moving front dominated injection tests. O'Sullivan and Pruess[5], and Garg[6] discussed the analysis of injection and falloff tests in two-phase geothermal reservoirs. These studies demonstrated that the pressure transients during injection tests can be used to determine the permeability thickness of the reservoir. Horne and Satman[7] proposed a method for estimating the distance to the thermal front from injection tests in two-phase reservoirs. The study by Benson and Bodvarsson[1] developed methods for calculating the skin factor from nonisothermal injection tests and discussed the conditions under which the pressure transients behaved like a composite reservoir or moving front dominated problem. The present study is an extension of this work.

SINGLE RATE ANALYSIS

The following analysis methods are applicable to a reservoir which is;
1) of uniform and constant porosity, compressibility, permeability, heat capacity and thermal conductivity;
2) horizontal, infinite, of constant thickness and bounded above and below by impermeable rock;
3) completely filled with slightly compressible liquid water; and
4) fully penetrated by a finite radius wellbore;
Under these conditions, single rate pressure transients are described by one of two cases; 1) a moving front dominated or 2) composite reservoir behavior. This is illustrated in Figure 1, where the pressure transients during 100°C injection into a 250°C reservoir are shown for four cases; injection into a hot reservoir and injection into a hot reservoir with pre-existing 1, 5 and 10 m cold spots.

Moving Front Dominated Problem

For injection with no pre-existing cold spot, pressure transients are initially identical to those of the hot (250°C) reservoir. After a period of time defined by

$$t_{oc} \approx \frac{\pi H r_w^2 e^{-2s}}{Q_c} ; \tag{1}$$

the pressure data fall on a new curve that has a slope corresponding to the properties of the injected fluid. Pressure transient data that are controlled by a moving thermal front can be analyzed by the following procedure. The permeability-thickness is calculated:

$$kH = 0.183 \frac{q \mu_c}{\rho_c m_c} ; \tag{2}$$

where m_c is the slope of the straight line on the P vs. log t plot that corresponds to the properties of the injected fluid. To determine P_{1s}, extrapolate m_c to 1 second. P_{1s} is then corrected to account for the offset between the isothermal and nonisothermal curves by

$$P^*_{1s} = P_{1s} + \Delta P_o ; \qquad (3)$$

where

$$\Delta P_o = \frac{q}{2\pi kH}\left[\frac{\mu_c}{\rho_c}P_D(t_{Doc})_c - \frac{\mu_h}{\rho_h}P_D(t_{Doc})_h\right]; \quad (4)$$

and

$$t_{Doc} = \frac{\pi H\rho_h}{q}\frac{k}{\phi\mu\beta_t} . \qquad (5)$$

The skin factor is then calculated

$$s = 1.151\left(\frac{P^*_{1s} - P_i}{m_c} - \log\frac{k}{\phi\mu_c\beta_t r_w^2} - .351\right). (6)$$

Note that if P_{1s} is not corrected to account for the offset between the isothermal and non-isothermal pressure transients, the skin factor will be underestimated.

Composite Reservoir Behavior

The three other curves in Figure 1 are the pressure transients in response to injection with pre-existing cold spots of 1, 5, and 10 m radii. For each case, the data are initially identical to isothermal 100°C injection. When

$$t_{oh} > \frac{\phi\mu_c\beta_t}{4k}r_c^2 \qquad (7)$$

the data changes to a new slope that corresponds to the reservoir fluid properties. This two-slope behavior is referred to as the composite reservoir problem. At even longer times the data again change slope and become identical to the moving front-dominated problem, this last transition occurs at

$$t'_{oc} \approx \frac{\rho_w c_w}{\rho_a c_a}\frac{\pi H r_c^2}{Q_c} . \qquad (8)$$

Care must be taken in the analysis of pressure data near this region because the transition begins 1/4-log cycle before this point and lasts for 1/2-log cycle after it. Data from the final slope are analyzed according to the moving-front procedure.

Pressure fall-off data (when the well is completely shut in) are always analyzed with a composite reservoir model because once the well is shut in, the thermal front moves forward at a negligible rate.

The permeability-thickness of the reservoir and the skin factor can be evaluated by the following procedure. The permeability-thickness is calculated

$$kH = .183\frac{q\mu_h}{\rho_h m_h} ; \qquad (9)$$

where m_h is the slope on the P vs. log t plot which corresponds to the properties of the reservoir fluid. P_{1s} is determined by extrapolating m_h to 1 second and correcting to account for the effect of the cold spot around the well:

$$P^*_{1s} = P_{1s} \pm .87\ m_h s_c; \quad \begin{array}{l}(+ \text{ fall-off,} \\ - \text{ injection})\end{array} \quad (10)$$

where

$$s_c = \left(\frac{\mu_c}{\mu_h}\frac{\rho_h}{\rho_c} - 1\right)\ln\left(\frac{r_c}{r_w}\right). \qquad (11)$$

The skin factor for the well is calculated by:

$$s = 1.151\left(\frac{\mu_h\rho_c}{\mu_c\rho_h}\right)\left[\frac{P^*_{1s} - P_{i\ or\ wf}}{m_h}\right.$$
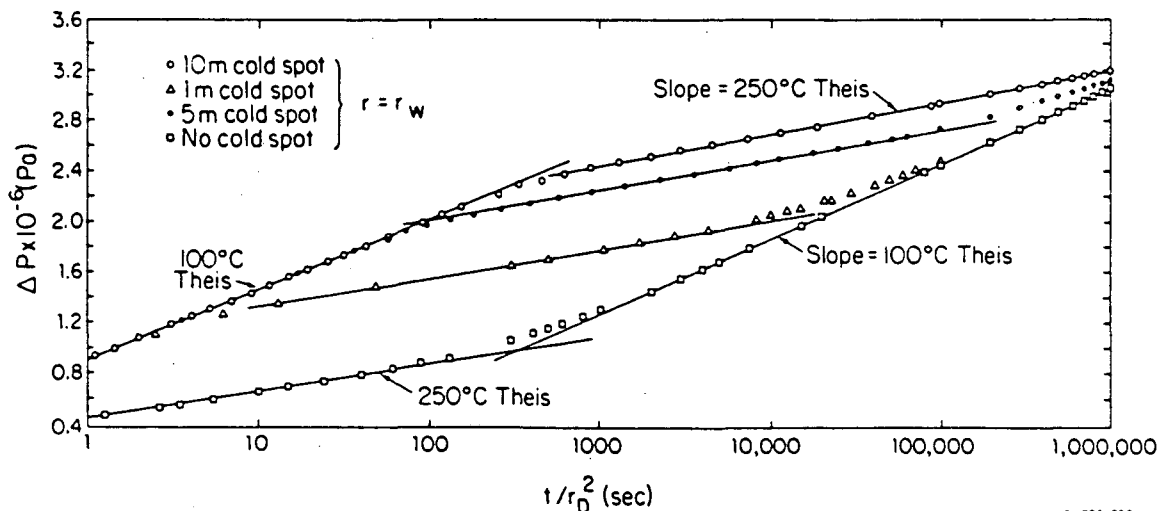$$\left. - \log\left(\frac{k}{\phi\mu_h\beta_t r_w^2}\right) - .351\right]. \qquad (12)$$

Figure 1. Pressure transient data for 100°C injection into a 250°C reservoir.

2

Relative to the hot reservoir, the effective skin factor is increased by a factor of $\mu_c \rho_h / \mu_h \rho_c$. If the skin value is calculated without considering the effect of the cold spot around the well, the skin factor will be grossly overestimated.

STEP RATE INJECTION TESTS

Typically, injection tests are not conducted at a single flow rate, but instead, conducted in a series of step rates followed or preceded by a complete shut in. Therefore, it is important to determine if the methods developed for single-rate tests can be adapted for the interpretation of step rate tests.

Approach

The computer code, PT, was used to simulate pressure transients during nonisothermal step-rate tests. PT employs the integrated finite-difference method to discretize the medium and formulate the mass and energy transport equations in a liquid-saturated porous medium[8,9]. The simulator allows both temperature and pressure-dependent fluid properties. These properties are computed internally to within 1% of their true values. A single-layer radial mesh with a realistic wellbore radius of 0.1 m radius was used. To accurately model the temperature changes during injection, very fine elements were used close to the well. Farther away, the spacing increased logarithmically. The outer boundary of the mesh was sufficiently distant to avoid any affect on the pressure transient data.
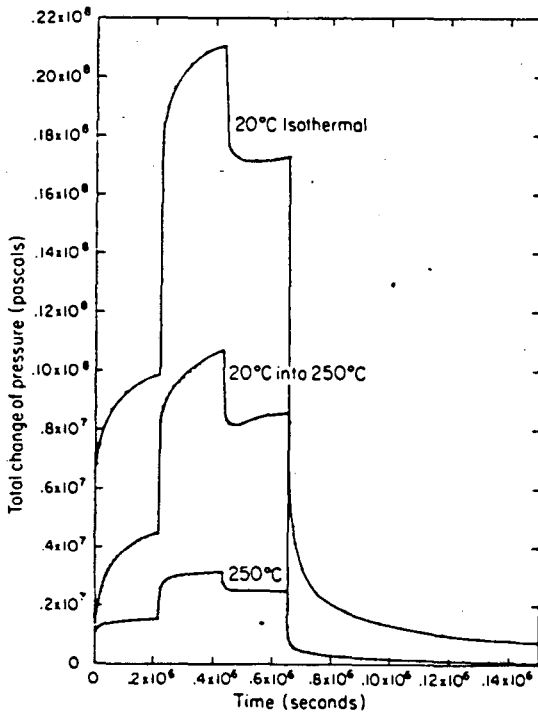

Fig. 2. Simulated pressure data from a step test with 20°C injection into a 250°C reservoir. Also shown are the simulated pressure data for isothermal 20°C and 250°C injection.

Simulated pressure data were then plotted in terms of

$$ P \text{ vs. } \sum_{i=1}^{n} \frac{q_i}{q_n} \log \frac{t_i + \cdots + t_n + \Delta t}{t_{i+1} + \cdots + t_n + \Delta t} ; \quad (14) $$

in accordance with conventional multirate theory[10]. From this plot, the permeability thickness can be calculated:

$$ kH = .183 \frac{q_n \mu}{\rho m} ; \quad (15) $$

where the appropriate μ, ρ and m are determined by procedures discussed in the the following sections. For the moving front problem the skin factor is determined by

$$ s = 1.151 \left[\left(\frac{q_n}{q_n - q_{n-1}} \right) \frac{P^*_{1s} - P_{wf}}{m_c} \right. $$
$$ \left. - \log \frac{k}{\phi \mu_c \beta_t r_w^2} - .351 \right] ; \quad (16) $$

and for the composite reservoir problem:

$$ s = 1.151 \frac{\mu_c \rho_h}{\mu_h \rho_c} \left[\left(\frac{q_n}{q_n - q_{n-1}} \right) \frac{P^*_{1s} - P_{wf}}{m_h} \right. $$
$$ \left. - \log \frac{k}{\phi \mu_h \beta_t r_w^2} - .351 \right] . \quad (17) $$

EXAMPLE

The following test was simulated to illustrate the key aspects of nonisothermal step rate injection tests. Three six-hour steps with injection rates of 0.1 kg/s/m, 0.2 kg/s/m and .15 kg/s/m of 20°C fluid into a 250°C reservoir were followed by a complete shut in. Table 1 summarizes the properties of the reservoir used for the simulation. The simulated pressure data are shown in Figure 2. For comparison, isothermal 20°C and 250°C injection are also plotted. Note that the magnitude of the non-isothermal pressure changes are intermediate between the two isothermal cases. For the first three steps, the shape of the curves are similar to the 20°C case, however, the fall-off data, except for the first few minutes, are identical to the 250°C case.

Pressure Transient Analysis

Step 1, a typical moving-front-dominated problem, is shown in Figure 3. Initially, the data are identical to the 250°C isothermal pressure transients (also shown in Figure 3). At approximately 300 seconds, the data depart from the initial curve and fall on a new slope which corresponds to the properties of the injected fluid. The data from 300 seconds to six hours can be analyzed to determine the permeability-thickness of the reservoir from Eq. 2 and the

3

skin factor from Eq. 6. Values of $kH = 10^{-14}$ m^3 and $s = 0.04$ are calculated; both are in excellent agreement with the input values of 10^{-14} m^3 and 0.0, respectively. If P_{1s} is not corrected to account for the offset between the isothermal and nonisothermal curves, a skin value of -3.5 is calculated.

Step 2, shown in Figure 4, first displays the composite reservoir behavior and then, the moving front-dominated behavior. The early transients are governed by the 0.64 m cold spot generated by Step 1. At approximately 4 s the pressure data changes to a slope which corresponds to the properties of the reservoir fluid. At approximately 1.1 hours the data depart from the second slope and the moving thermal front controls the pressure response. The transition times are in good agreement with those calculated from Eq. 7 and Eq. 8, $t_{oh} \approx 3$ s and $t_{oc}' \approx$ 1.2 hours, respectively. It is apparent that superposition is an appropriate manner in which to treat this problem and that the equations developed for single-rate tests are valid if the effect of the growing cold spot is taken into consideration.

Data from step 2 may be difficult to analyze because wellbore storage may mask most of the data from the first and second slope. Also, the third slope will be clearly defined for less than one-half of a log cycle. If however, the second slope is apparent, the permeability thickness can be evaluated by Eq. 15 and the skin factor evaluated by Eq. 17. Values of 10^{-14} m^3 and -0.2 are obtained; these are in good agreement with the input values. The slight negative skin is calculated as a result of the approximation

$$r_c^2 \approx r_{tf}^2 = \frac{\rho_w c_w}{\rho_a c_a} \frac{Q}{\pi H} .$$ (18)

An apparent skin value, the skin factor relative to the hot reservoir can be calculated:

$$s_a = 1.151 \left[\left(\frac{q_n}{q_n - q_{n-1}} \right) \frac{P_{1s} - P_{wf}}{m_h} \right.$$

$$\left. - \log \frac{k}{\phi \mu_h \beta_t r_w^2} - .351 \right] .$$ (19)

For step 2, the apparent skin factor is 14 (compared to a true skin value of 0.0), indicating that the cold spot around the well contributes a significant component to the pressure buildup.

Step 3 begins at 12 hours into the test. By this time the thermal front has advanced 1.75 m into the formation. Equation 7 indicates that the reservoir will behave as a composite system until 11.4 hours after the rate change. Therefore, the entire 6-hour step will only reflect the composite reservoir behavior. This is clearly shown in Figure 5 where only two slopes are apparent, the first corresponding to the fluid properties of the cold spot and the sec-

ond, to the reservoir fluid. The second slope can be used in conjunction with Eq. 15 to calculate the permeability-thickness of the reservoir. The skin factor, calculated from Eq. 17, is equal to -0.04. The apparent skin factor, calculated from Eq. 19, is 18.9.
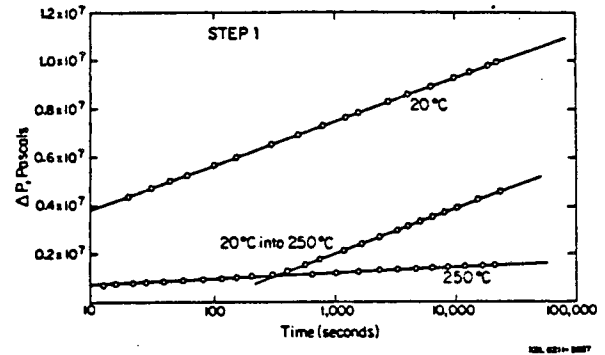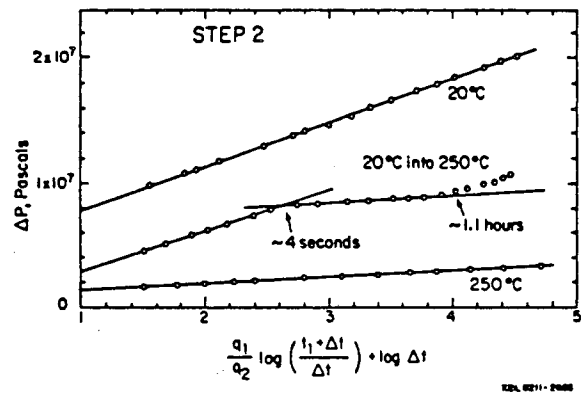

Fig. 3. Pressure vs. log t plot for step 1.

Fig. 4. Simulated pressure data from step 2.

Table 1   Reservoir Properties Used for Step Rate Simulation.

k	1.0×10^{-14} m^2
H	1.0 m
ϕ	0.2
c_r	1000.0 J/kg·°C
ρ_r	2200.0 kg/m³
λ	2.0 J/m·°C·s
r_w	0.1 m
β_t	1.0×10^{-9} Pa^{-1}

Fall-off

The pressure falloff data following the step test are plotted in Figure 6. As expected, the data initially follow a slope corresponding to the properties of the cold spot and then become identical to the pressure fall-off data for 250°C isothermal injection. The data after 35 s can be used to calculate a kH of 10^{-14} and a skin value (from Eq. 17) of -0.2. The apparent skin factor (from Eq. 19) is 19.8.

Injectivity

It is interesting to note that the well injectivity, shown in Figure 7, is of little value for the inference of downhole well productivity. This results from the lack of an obvious relationship between the nonisothermal injectivity (middle curve) and the two isothermal cases (from which, theoretically, productivity could be inferred).

DISCUSSION

The previous analysis demonstrated the pressure transient response to nonisothermal step-rate tests. In the early steps, both the moving front-dominated and composite reservoir behavior were observed. During the last two steps, the pressure transient behaved like a composite reservoir. It is of importance to note that in this example the transmisivity (kH/μ) varied by a factor of ten during the step test, creating an apparent increase in the permeability-thickness, if misinterpreted.

It is possible to calculate the correct permeability-thickness of the formation from the pressure transient data if the fluid properties to which the slope corresponds can be determined. This can be determined by evaluating Eqs. 7 and 8. True skin factors can also be calculated from Eqs. 16 or 17. However, once the reservoir behaves as a composite system, it is important to have a reasonable estimate of the reservoir thickness and injection history from which the distance to the thermal front can be estimated. If these are not well known, it is not possible to calculate the skin factor with Eq. 17. On the other hand, it is possible to calculate the apparent skin factor from Eq. 19. Also, recall that the apparent skin factor increased from 14 to nearly 20 over the 18-hour step test discussed in the previous section. Since the apparent skin factor of the well is only a function of the true skin, the size of the cold spot and the contrast between the properties of the injected and in-situ fluid, and, if we assume that the true skin factor of the well does not change over the test period, then the growth in the apparent skin factor is a reflection of the growth of the cold spot. This relationship can be used as the basis of a procedure for estimating the true skin factor and size of the cold spot.

If the radius of the cold spot is less than $100 \times r_w$, then the cold spot around the well can be treated as the thermal skin where
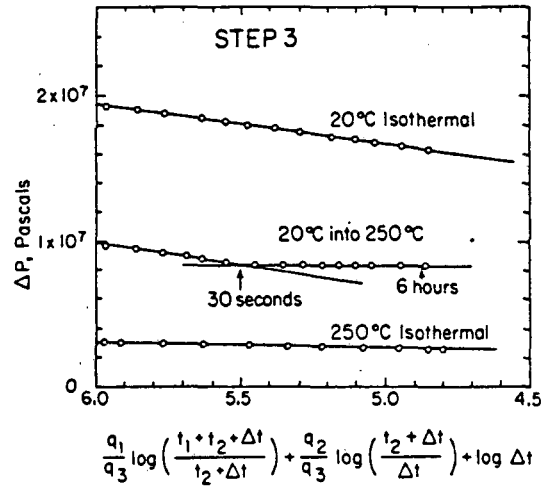

$$\frac{q_1}{q_3} \log\left(\frac{t_1+t_2+\Delta t}{t_2+\Delta t}\right) + \frac{q_2}{q_3} \log\left(\frac{t_2+\Delta t}{\Delta t}\right) + \log \Delta t$$

XBL 8211-2665

Fig. 5. Simulated pressure data from step 3.

$$\frac{q_1}{q_3} \log\left(\frac{t_1+t_2+t_3+\Delta t}{t_2+t_3+\Delta t}\right) + \frac{q_2}{q_3} \log\left(\frac{t_2+t_3+\Delta t}{t_3+\Delta t}\right) + \log\left(\frac{t_3+\Delta t}{\Delta t}\right)$$
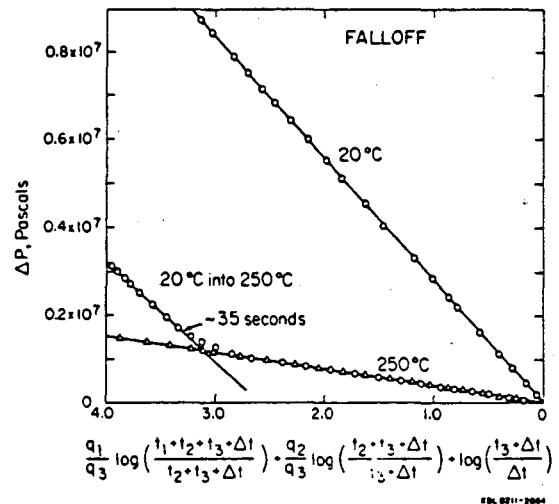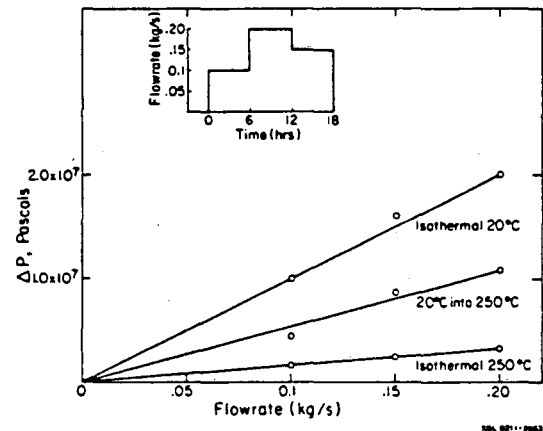
Fig. 6. Simulated pressure data from step 4 (falloff).

Fig. 7. Injectivity data from the simulated step test.

$$s_c = \left(\frac{\mu_c \rho_h}{\mu_h \rho_c} - 1 \right) \ln \left(\frac{r_c}{r_w} \right); \qquad (20)$$

as the cold spot grows, so does s_c. The size of the cold spot can be calculated from

$$r_c \approx r_{tf} = \sqrt{ \frac{\rho_w c_w}{\rho_a c_a} \frac{C}{\pi H} } . \qquad (21)$$

If this is substituted into Eq. 20, we find that

$$s_c = 1.151 \left(\frac{\mu_c \rho_h}{\mu_h \rho_c} - 1 \right) \left[\log C + \log \frac{\rho_w c_w}{\rho_a c_a} \frac{1}{\pi H r_w^2} \right]. \qquad (22)$$

Therefore, on a plot of s_a vs. log C, the points should fall on a single straight line with a slope of

$$n = 1.151 \left(\frac{\mu_c \rho_h}{\mu_h \rho_c} - 1 \right) . \qquad (23)$$

Extrapolating n to a cumulative injection of $\pi r_w^2 H$, the point at which no cold fluid has been injected into the formation, s_{aw} can be evaluated. Recalling Eq. 12, one can determine that

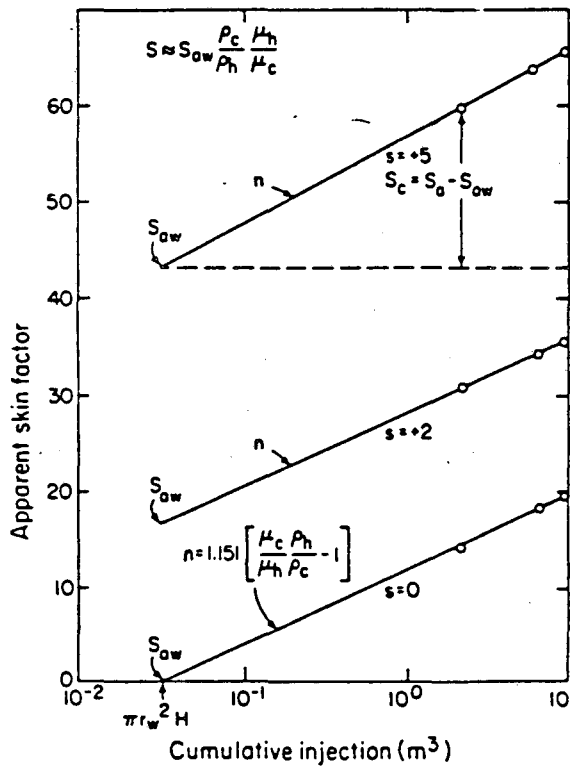$$s = s_{aw} \frac{\mu_h \rho_c}{\mu_c \rho_h} . \qquad (24)$$

Fig. 8. Apparent skin vs. log C for three skin values, 0,2 and 5.

Knowing s_{aw}, the thermal skin effect s_c can be calculated

$$s_c = s_a - s_{aw} ; \qquad (25)$$

and the distance to the cold spot can be calculated

$$r_c = r_w e^{\left(\frac{1.151 s_c}{n} \right)} . \qquad (26)$$

The apparent skin factors calculated for the step-rate test discussed in the previous section are plotted in Figure 8, as a function of the cumulative injection. Also plotted, are data from similar step tests where the true skin values of the well are 2 and 5 respectively. Note that the slope of the line is identical in each case and is equal to $1.151(\mu_c \rho_h / \mu_h \rho_c - 1)$. The values of the skin factor calculated from Eq. 24 are, 0, 2.0, and 5.2, respectively. Similarly, using Eq. 26, the distance to the cold front can be estimated at each of the three values of s_a. The calculated values are 0.65 m, 1.20 m, and 1.55 m compared to the correct values of 0.7 m, 1.3 m, and 1.6 m, respectively. Both the calculated skin factors and distances to the thermal front are in excellent agreement with their true values.

The procedure described in the above section does not require a step-rate test but simply any pressure transient data (such as fall-off) after increasing quantities of injection. The procedure is useful not only in determining the effect of the growing cold spot around the well but also can be used to detect true damage or enhancement of a well. If the slope of the semilog line n, is greater or less than its expected value, then changes in the apparent skin factor must be caused by true damage to or enhancement of the near-wellbore region.

The analysis methods discussed and developed here are applicable to porous medium reservoirs where the movement of a thermal front can be described in terms of a t/r^2 relationship. Extension of these methods to fractured systems will require consideration of both the t/r^2 and t/r^4 dependence typical of fracture systems[2]. Also inherent to this analysis is the assumption that the compressibility of the fluid is nearly equal on both sides of the thermal front. In other words, these methods are not directly applicable to two-phase or dry steam reservoirs.

CONCLUSIONS

1) The methods developed for the interpretation of single-rate nonisothermal injection tests in conjunction with conventional multi-rate analysis methods are applicable to step-rate tests.

2) The generalization that pressure transients during injection are controlled by the properties of the injected fluid is not applicable to step rate tests.

3) Apparent skin factors (relative to the hot reservoir) can be used to calculate the true skin factor of the well and the distance to the thermal front.

4) Nonisothermal injection tests must be carefully designed to obtain data with clearly defined pressure transients which correspond to either the moving-thermal-front or composite-reservoir problem.

ACKNOWLEDGEMENTS

NOMENCLATURE

c	heat capacity (J/kg°C)
C	cumulative injection (m^3)
H	reservoir thickness (m)
k	permeability (m^2)
m	absolute value of the slope on a P vs. log t plot (Pa/cycle)
n	slope on an s_a vs. log C plot (m^{-3})
P	pressure (P_a)
P_{1s}	extrapolated pressure at 1s on a P vs. log t plot (Pa)
P_{1s}^{*}	corrected pressure at 1s (Pa)
P_D	dimensionless pressure
P_i	initial pressure (Pa)
P_{wf}	flowing pressure (Pa)
q	mass flow rate (kg/s)
Q	volumetric flow rate (m^3/s)
r	radius (m)
s	skin
s_a	apparent skin
s_c	thermal skin
s_{aw}	apparent skin evaluated at $\pi r w^2 H$
t	time (s)
t_{oc}	time at which the hot and cold slopes intersect for injection with no initial cold spot.
t_{oc}'	time at which the hot and cold slope intersect for injection with a pre-existing cold spot.

Greek Letters

β_t	total compressibility (Pa^{-1})
ϕ	porosity
μ	dynamic viscosity (Pa·s)
ρ	density (kg/m^3)

Subscripts

a	reservoir
c	cold
D	dimensionless
h	hot
n	index for flowrate step
tf	thermal front
w	water

REFERENCES

1. Benson, S.M. and Bodvarsson, G.S.: "Non-isothermal Effects During Injection and Falloff Tests," SPE paper 11137, presented at the 57th Annual Meeting of the Society of Petroleum Engineers, New Orleans, Louisiana, 1982.

2. Bodvarsson, G.S. and Tsang, C.F.: "Thermal Effects in the Analysis of Fractured Reservoirs" in 3rd Invitational Well Testing Symposium, Lawrence Berkeley Laboratory Report, LBL-12076, Berkeley, California, March, 1980.

3. Mangold, D.C., Tsang, C.F., Lippmann, M.J., and Witherspoon, P.A.: "A Study of Thermal Discontinuity in Well Test Analysis," Journal of Petroleum Technology (June, 1981), v. 33, No. 6.

4. Tsang, Y.W., and Tsang, C.F.: "An Analytic Study of Geothermal Reservoir Pressure Response to Cold Water Reinjection," in Proceedings 4th Workshop on Geothermal Reservoir Engineering, December, Stanford University, Stanford, California.

5. O'Sullivan, M.J., and Pruess, K.: "Analysis of Injection Testing of Geothermal Reservoirs," Geothermal Resources Council Transactions, vol. 4, 1980.

6. Garg, S.K.: "Pressure Transient Analysis for Two-phase (Liquid Water/Steam) Geothermal Reservoirs," SPE 7479, presented at the SPE 53rd Annual Meeting, Houston, Texas, (October 1-3, 1978).

7. Horne, R. N., and Satman, A.: "A Study of Drawdown and Buildup in Wells with Phase Boundaries," Geothermal Resources Council Transactions, vol. 4, 1980.

8. Edwards, A.L.: "TRUMP: A Computer Program for Transient and Steady State Temperature Distribution in Multidimensional Systems, Lawrence Livermore Laboratory, Livermore, California, UCRL-14754, Rev. 3, 1972.

9. Bodvarsson, G.S.: "Mathematical Modeling of the Behavior of Geothermal Systems Under Exploitation," Ph.D. dissertation, University of California, Berkeley, 1981.

10. Earlougher, Jr., R.C.: Advances in Well Test Analysis, Society of Petroleum Engineers, Monograph 5, 1977.